

# Properties of the temporal transfer matrix in integrable Floquet circuits

Ilya Vilkoviskiy<sup>1,2</sup> and Kirill Matirko<sup>3</sup>

<sup>1</sup>Department of Theoretical Physics, University of Geneva, Quai Ernest-Ansermet 30, 1205 Geneva, Switzerland

<sup>2</sup>Department of Physics, Princeton University, Princeton NJ 08544, USA

<sup>3</sup>Department of Mathematics, HSE University, Moscow 119048, Russia

August 21, 2025

## Abstract

One possible approach to studying non-equilibrium dynamics is the so-called influence matrix (IM) formalism. The influence matrix can be viewed as a quantum state that encodes complete information about the non-equilibrium dynamics of a boundary degree of freedom. It has been shown that the IM is the unique stationary point of the temporal transfer matrix. This transfer matrix, however, is non-diagonalizable and exhibits a non-trivial Jordan block structure.

In this article, we demonstrate that, in the case of an integrable XXZ spin chain, the temporal transfer matrix itself is integrable and can be embedded into a family of commuting operators. We further provide the exact expression for the IM as a particular limit of a Bethe wavefunction, with the corresponding Bethe roots given explicitly.

We also focus on the special case of the free-fermionic XX chain. In this setting, we uncover additional local integrals of motion, which enable us to analyze the dimensions and structure of the Jordan blocks, as well as the locality properties of the IM. Moreover, we construct a basis of quasi-local creation operators that generate the IM from the vacuum state.

## 1 Introduction

Understanding the universality classes of correlation functions in quantum systems is one of the central goals of quantum many-body physics. While ground-state properties are comparatively well understood, real-time correlations remain challenging. Integrable models provide a uniquely controlled setting. On the microscopic side, form-factor expansions yield exact expressions for dynamical correlation functions [1–3]. In practice, however, these methods are most effective for two-point functions and become hard to extend to higher-point or long-time regimes.

At the opposite, coarse-grained end, generalized hydrodynamics (GHD) captures Euler-scale transport and post-quench evolution of local observables [4, 5]. GHD organizes late-time dynamics in terms of quasiparticle densities and their effective velocities, providing predictions for transport coefficients and hydrodynamic tails. Yet refined phenomena such as KPZ-type dynamical scaling [6] and the systematic computation of correlation functions in the presence of weak integrability breaking are still not fully understood, see [7] for discussion.

A natural way to bridge these microscopic and hydrodynamic descriptions is through controlled real-time simulations that preserve integrability. Integrable Floquet dynamics offer precisely such a playground: they implement exact, stroboscopic time evolution within an integrable framework, enabling direct access to space-time dependent correlators, finite-density quenches, and scaling crossovers beyond the strict Euler scale [8–11].

In this work, we introduce a framework, inspired by the so-called influence matrix (IM) approach to dynamical Floquet systems, introduced in [12]. The IM is a quantum state that encodes complete information about the non-equilibrium dynamics of a boundary degree of freedom. It has been shown that the IM is the unique stationary point of the temporal transfer matrix. This transfer matrix, however, is non-diagonalizable and exhibits a non-trivial Jordan block structure. It was reported that, at least close to the vicinity of a special exactly solvable dual-unitary (DU) point, the IM exhibits a logarithmic growth of temporal entanglement entropy [13], formulating a conjecture that it might be a generic feature for the XXZ integrable system. Our framework is similar to the one introduced in [14], where the authors studied correlation functions of a boundary spin in a brick-wall Floquet dynamics. However, in our approach, correlation functions are computed by sandwiching local observables between two IMs utilizing the logarithmic entanglement, instead of a trace calculation in [14] which demands the knowledge of the whole spectrum of the temporal transfer matrix.

We introduce a family of commuting transfer matrices  $T(v)$  corresponding to the XXZ model with four alternating inhomogeneities and  $4N$  sites, where  $2N$  is the number of time steps of a Floquet dynamics. These transfer matrices commute with the temporal transfer matrix; therefore, the IM itself can be considered as a Bethe vector. Remarkably, we have found that the Bethe vector corresponding to the IM has very specific and explicit Bethe roots, provided by the exact solution of Bethe ansatz equations (BAE). Our approach differs from the quantum transfer matrix (QTM) formalism introduced in [15] and adapted for dynamical observables in [16]. The QTM method is formulated specifically in the continuous-time limit and requires taking a careful scaling limit to recover physical dynamics. While our setup can also be tuned toward a continuous-time regime, the integrable structure we construct defines a local Floquet evolution with a finite number of time steps. This leads to novel spectral and quasiparticle properties of the temporal transfer matrix.

Similarly to [14], we observed that the transfer matrix is non-diagonalizable. This non-diagonalizability can be explained on the level of quasiparticles. We observed massive quasiparticles related to spin-one excitations, and also light quasiparticles with Bethe roots concentrated around one of the four inhomogeneities of the transfer matrix. The light quasiparticles are responsible for the Jordan block structure. On a single-particle level, each of the four types of quasiparticles corresponds to a different Jordan block of size  $N$ . On the many-body level, each quasiparticle either belongs to a spin-one sector or to one of the four Jordan blocks in a spin-zero sector. The IM corresponds to a state with no spin-one particles and two Jordan blocks fully occupied, while the other two are empty. Quasiparticles, however, do not correspond to local excitations and have rather long-range support.

The analysis of an integrable system typically begins with the study of the spectrum of its transfer matrix. In the degenerate case, the corresponding characterization is given by the degeneracies and the structure of its Jordan blocks. These features have not been systematically explored; here we take a first step toward filling this gap. Our results offer a fresh perspective on integrable dynamical systems. Moreover, the influence-matrix (IM) machinery extends beyond correlation functions, as it can also address quantum quenches and dynamics in the presence of an integrability-breaking impurity. We hope this framework will open a practical route to study these phenomena efficiently.

In order to better understand the structure of Jordan blocks, we analyzed the free-fermionic XX limit. Remarkably, we have found the local non-Hermitian Hamiltonians that commute with the transfer matrix  $T(v)$ , and have the IM as a unique ground state with zero energy. Due to non-Hermiticity, these Hamiltonians share the same Jordan block structure as the transfer matrix. We note that a similar structure was studied in [17] in the context of third quantization of Lindbladian dynamics and the Jordan blocks were provided by [18]. Thus, our model provides an interesting and unexpected playground to study the non-Hermitian physics. We provide the canonical Jordan form of the local Hamiltonians and the transfer matrix on the single-particle sector and then, following [18], study the distribution of the Jordan block sizes, reporting exponentially many blocks of thermodynamically large size. Such a distribution is expected for the temporal transfer matrix, and is responsible for the entanglement barrier reported in [19, 20].

Instead, we observed that in the free fermionic limit, the special linear combinations of quasiparticles can be localized up to power-law tails. We observed that this basis can be found by the Gram-Schmidt orthogonalization procedure of the Jordan block basis. The existence of a basis with power-law tails provides us with a gapped quasi-

local Hamiltonian  $H_{\text{gap}}$  with the tails decaying according to the power law  $r^{-3/2}$ , confirming a similar observation in the case of the kicked Ising model at an integrable point [21].

## 2 IM approach to Floquet dynamics

**Brick-wall Floquet dynamics, and IM** Let us consider an infinite spin chain  $\mathbb{H} = \cdots \mathbb{V}_{-2} \otimes \mathbb{V}_{-1} \otimes \mathbb{V}_0 \otimes \mathbb{V}_1 \otimes \mathbb{V}_2 \dots$ , where each space  $\mathbb{V}_s$  is isomorphic to  $\mathbb{C}^2$ . The chain is equipped with two-qubit gates  $U_{i,i+1}$  - unitary operators acting non-trivially only on the  $i$ -th and  $(i+1)$ -th spins. We define two evolution operators  $U_{\text{odd}} = \prod_{i=-\infty}^{\infty} U_{2i-1,2i}$ ,  $U_{\text{even}} = \prod_{i=-\infty}^{\infty} U_{2i,2i+1}$ , and their product  $U = U_{\text{even}}U_{\text{odd}}$ . This unitary operator sets a non-trivial dynamics that might be thought of as a Trotterization [10] of the XXZ dynamics [22, 23]. In this article, we will study the approach of the influence matrix (IM), and discover the structures of integrability in this case. Let us define the half-chain operators:  $U_{\text{odd}}^+ = \prod_{i=-\infty}^0 U_{2i-1,2i}$ ,  $U_{\text{even}}^+ = \prod_{i=-\infty}^{-1} U_{2i,2i+1}$ , and their product  $U^+ = U_{\text{even}}^+U_{\text{odd}}^+$ . The IM is a functional that takes values on the trajectories of a boundary spin and is defined as follows:

$$\mathcal{I}_s^{\bar{s}} = \text{tr} \left( \langle \bar{s}_{2N-1} | (U^+)^{-1} | \bar{s}_{2N-2} \rangle \dots \langle \bar{s}_3 | (U^+)^{-1} | \bar{s}_2 \rangle \langle \bar{s}_1 | (U^+)^{-1} | \bar{s}_0 \rangle \rho_b \langle s_0 | U | s_1 \rangle \langle s_2 | U | s_3 \rangle \dots \langle s_{2N-2} | U | s_{2N-1} \rangle \right), \quad (2.1)$$

here the trace is taken over all the spaces  $\mathbb{V}_i$  for  $i > 0$ , and we choose the density matrix in the bulk as:

$$\rho_b = \frac{q^{\sigma_z}}{q + q^{-1}} \otimes \frac{q^{\sigma_z}}{q + q^{-1}} \otimes \dots \quad (2.2)$$

The IM contains the information about correlation functions of arbitrary local operators. For any operator  $\mathcal{O}_0$ , define  $\mathcal{O}_0(2N) = U\mathcal{O}_0U^{-1}$ , the trace of this operator can be computed by sandwiching between two IMs:

$$\langle \mathcal{O}_0(2N) \rho_0 \rangle = \sum_{s_i \bar{s}_i} (\mathcal{I}_r)_{s_1, \dots, s_{2N}}^{\bar{s}_1, \dots, \bar{s}_{2N}} (\mathcal{I}_l)_{s_2, \dots, s_{2N+1}}^{\bar{s}_2, \dots, \bar{s}_{2N+1}} \rho_{s_1, \bar{s}_1} \mathcal{O}_{s_{2N+1}, \bar{s}_{2N+1}}. \quad (2.3)$$

here  $\mathcal{I}_l$  is given by the same formula as in 2.1, while  $\mathcal{I}_r$  is constructed in the same manner, for the evolution operator corresponding to the semi-infinite bath from the left.

Let us vectorize the IM, treating it as a vector. Eq. (2.3) might be rewritten in a bra-ket notation:

$$\langle \mathcal{I}_l | \mathcal{O}_0^\perp(2N) \rho_1^\perp | \mathcal{I}_r \rangle, \quad (2.4)$$

where  $\mathcal{O}_0^\perp(2N) = \mathcal{O}_{s_{2N+1}, \bar{s}_{2N+1}}$  - is an operator acting on a temporal  $2N+1$  site, and  $\rho_1^\perp = \rho_{s_1, \bar{s}_1}$  - is an operator acting on a temporal site 1. Note that left and right IM may have a different initial state  $\rho_b$  allowing us to study the quench dynamics. Another possible application - is to consider left and right IMs corresponding to different integrable systems (for example, systems with different anisotropy  $\Delta$ ). In this case, the correlator (2.4) corresponds to a non-integrable dynamics, but still can be calculated from the integrable data.

As we argue in this text, the temporal approach allows one to treat the IM as a special Bethe vector, effectively translating dynamical correlations into static ones with a particular Bethe vector. Before we proceed to define integrability, let us mention a few important properties of the IM.

**Causality light cone** It turns out that to consider dynamics up to  $2N$  time steps, it suffices to consider a bath on  $2N$  sites, as sites beyond this range do not influence the dynamics. The latter proof could be readily illustrated pictorially.

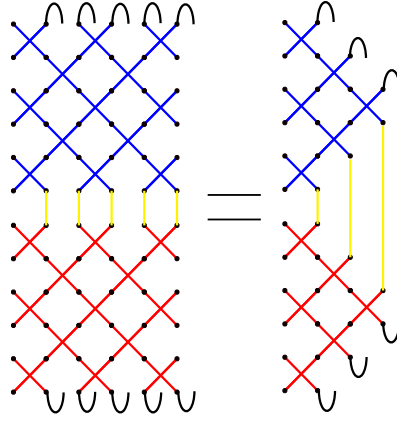


Figure 1: Pictorial representation of the IM, operators  $U$  are depicted in blue, while  $U^{-1}$  are in red.

And we used the identity  $U_{i,i+1}U_{i,i+1}^{-1} = Id$

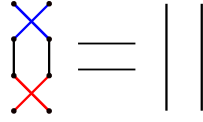


Figure 2: Pictorial representation of the identity  $U_{i,i+1}U_{i,i+1}^{-1} = Id$ .

## 2.1 Causality and Physicality

Let us enlist certain properties of the IM. First, using the Choi operator-state duality, one may consider the  $\mathcal{I}_{\mathbf{s}}^{\bar{\mathbf{s}}}$  as a density matrix of a certain state:

$$(\rho^{\mathcal{I}})_{\mathbf{s}}^{\bar{\mathbf{s}}} = 2^{-2N} \mathcal{I}_{\mathbf{s}}^{\bar{\mathbf{s}}}. \quad (2.5)$$

This means that the IM can be considered as an operator, which is positive with the trace equal to one. Another property is a reduction:

$$\sum_{s_n = \bar{s}_n} \mathcal{I}_{s_1, \dots, s_n}^{\bar{s}_1, \dots, \bar{s}_n} = \delta_{s_{n-1}, \bar{s}_{n-1}} \mathcal{I}_{s_1, \dots, s_{n-2}}^{\bar{s}_1, \dots, \bar{s}_{n-2}}. \quad (2.6)$$

This second property reflects the causality principle: measurements at later times cannot affect the dynamics at earlier times.

**Temporal transfer matrix** It is always possible to introduce a temporal transfer matrix  $\mathcal{T}$ , such that it stabilizes the IM:  $\mathcal{T}[\mathcal{I}] = |\mathcal{I}\rangle$ . Pictorially, one can define it as follows:

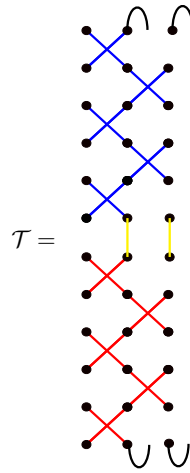


Figure 3: The graphical definition of the transfer matrix.

Properties (2.5),(2.6) have their counterpart at the level of the transfer matrix. Namely, one can ensure that the temporal transfer matrix maps influence matrices to influence matrices.

### 3 Yang-Baxter relation and auxiliary transfer matrix.

In this article, we restrict ourselves to the special class of unitaries  $U_{i,i+1}$  - which are given by an  $XXZ$   $R$ -matrix:

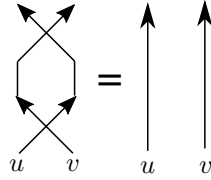
$$R_{i,i+1}(u) = \begin{pmatrix} 1 & 0 & 0 & 0 \\ 0 & \frac{\sinh(u)}{\sinh(u+\eta)} & \frac{\sinh(\eta)}{\sinh(u+\eta)} & 0 \\ 0 & \frac{\sinh(\eta)}{\sinh(u+\eta)} & \frac{\sinh(u)}{\sinh(u+\eta)} & 0 \\ 0 & 0 & 0 & 1 \end{pmatrix}_{i,i+1} \quad (3.1)$$

In this section, we construct an integrable transfer such that IM will be the eigenvector with the highest eigenvalue 1. Before we do so, let us prepare some notations. First of all, it is convenient to equip every line with a spectral parameter. On the intersection of two lines with the so-called spectral parameters  $u$  and  $v$  we put an  $R$ -matrix depending on their difference  $R(u-v)$ . These conventions are illustrated in the figures below:

$$R(u-v) = \begin{array}{c} \nearrow \\ \nwarrow \\ u \quad v \end{array} \quad (3.2)$$

$$\begin{array}{c} \text{red } X \\ \text{blue } X \end{array} = \begin{array}{c} \nearrow \\ \nwarrow \\ u \quad 0 \end{array} \quad \begin{array}{c} \text{blue } X \\ \text{red } X \end{array} = \begin{array}{c} \nearrow \\ \nwarrow \\ 0 \quad u \end{array} \quad (3.3)$$

The unitarity condition simply rewrites as:


 Figure 4: Unitarity condition in an  $R$ -matrix notations.

The nice property of the  $R$ -matrix is of course the Yang-Baxter relation:

$$R_{1,2}(v_1 - v_2)R_{1,3}(v_1 - v_3)R_{2,3}(v_2 - v_3) = R_{2,3}(v_2 - v_3)R_{1,3}(v_1 - v_3)R_{1,2}(v_1 - v_2), \quad (3.4)$$

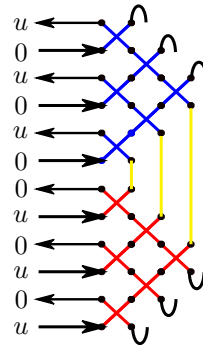
or after the transposition with respect to site  $i$ :

$$R_{1,2}(v_1 - v_2)R_{2,3}^{t_3}(v_2 - v_3)R_{1,3}^{t_3}(v_1 - v_3) = R_{1,3}^{t_3}(v_1 - v_3)R_{2,3}^{t_3}(v_2 - v_3)R_{1,2}(v_1 - v_2). \quad (3.5)$$

The latter can be depicted pictorially as follows:

(3.6)

Now we may equip our pictorial definition of the IM 3 with arrows and spectral parameters:



(3.7)

It is then natural to consider the following transfer matrix:

$$T(v) = \text{tr}_0 \left( R_{4N,0}(u-v) R_{0,4N-1}^{t_{4N-1}}(-v) \dots R_{2N+2,0}(u-v) R_{0,2N+1}^{t_{2N+1}}(v) \times \right. \\ \left. \times \rho_0(q) R_{2N,0}(-v) R_{0,2N-1}^{t_{2N-1}}(v-u) \dots R_{2,0}(-v) R_{0,1}^{t_1}(v-u) \right), \quad (3.8)$$

here  $\rho_0(q) = \frac{q^{\sigma_0^z}}{q+q^{-1}}$ . The pictorial definition of the transfer matrix is simple:


(3.9)

Note that the transfer matrix is a completely auxiliary object, at first glance it has nothing to do with the IM. We see, however, that the IM is an eigenvector of  $T(v)$  with eigenvalue one.

The proof is very simple and could be done pictorially:

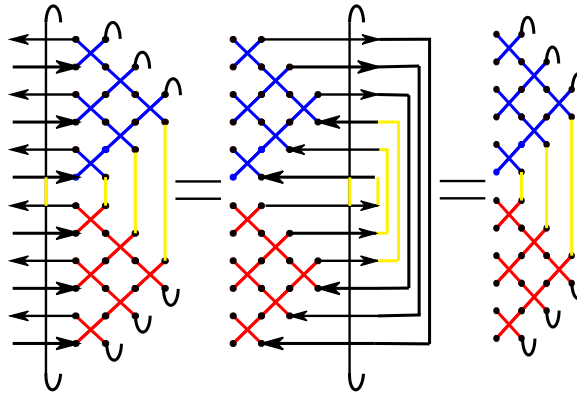


Figure 5: Definition of  $T$  and pictorial proof of the equation  $T|\mathcal{I}\rangle = |\mathcal{I}\rangle$ .

In the first identity, we used Yang-Baxter (3.5), while in the second identity, we used the unitarity condition (4).

Our goal for this article is to develop the Bethe ansatz techniques for the influence matrix.

The nice property is that (3.4),(3.5) implies the commutation of transfer matrices of different arguments:

$$[T(v_1), T(v_2)] = 0. \quad (3.10)$$

The commutativity again follows from the Yang-Baxter relations (3.4),(3.5). As we show later, the transfer matrices are not diagonalizable; they rather contain Jordan blocks. However, the eigenvector with the highest eigenvalue 1 is unique and can be found analytically.

**Crossing relation, equivalent transfer matrix, degenerate modules.** In order to get rid of unpleasant transpositions, and bring the transfer matrix to the more convenient form, we use the crossing relation:

$$R_{k,0}^{t_k}(-v) = \frac{\sinh(v)}{\sinh(v-\eta)} \sigma_k^y R_{0,k}(v-\eta) \sigma_k^y. \quad (3.11)$$

After the additional transposition over the auxiliary site 0 and the conjugation by an operator  $\prod_{i=1}^{2N} \sigma_{2i-1}^y$ , the transfer matrix in 3.8 is similar to the following matrix  $\tilde{T}(v)$ :

$$\tilde{T}(v) = \left( \frac{\sinh(v)}{\sinh(v-\eta)} \right)^N \left( \frac{\sinh(v-u)}{\sinh(v-u-\eta)} \right)^N \text{tr}_0 \left( R_{0,1}(v-u) R_{0,2}(v-\eta) \dots R_{0,2N-1}(v-u) R_{0,2N}(v-\eta) \times \right. \\ \left. \times \rho_0(q^{-1}) R_{0,2N+1}(v) R_{0,2N+2}(v-u-\eta) \dots R_{0,4N-1}(v) R_{0,4N}(v-u-\eta) \right). \quad (3.12)$$

Now it should be clear why the transfer matrix is not diagonalizable. Indeed, it can be seen that the product of two  $R$ -matrices with spectral parameters shifted by  $\eta$  has an invariant subspace. This can be seen directly from the Yang-Baxter equation:

$$R_{1,2}(\eta) R_{0,1}(v) R_{0,2}(v-\eta) = R_{0,2}(v-\eta) R_{0,1}(v) R_{1,2}(\eta). \quad (3.13)$$

One can note that  $R_{1,2}(\eta)$  is nothing but a projector onto the symmetric subspace. Thus, we obtain that the product  $R_{0,2}(v-\eta) R_{0,1}(v)$  has an invariant symmetric subspace, while the product in the opposite order  $R_{0,1}(v) R_{0,2}(v-\eta)$  has a singlet (anti-symmetric) subspace as a kernel.

## 4 Bethe ansatz

In order to use the standard Bethe ansatz technique, let us resolve the degeneracy by slightly shifting the spectral parameters.

$$\tilde{T}_\epsilon(v) = \left( \frac{\sinh(v)}{\sinh(v-\eta)} \right)^N \left( \frac{\sinh(v-u)}{\sinh(v-u-\eta)} \right)^N \text{tr}_0 \left( R_{0,1}(v-u) R_{0,2}(v-\eta-\epsilon) \dots R_{0,2N-1}(v-u) R_{0,2N}(v-\eta-\epsilon) \times \right. \\ \left. \times \rho_0(q^{-1}) R_{0,2N+1}(v) R_{0,2N+2}(v-u-\eta-\epsilon) \dots R_{0,4N-1}(v) R_{0,4N}(v-u-\eta-\epsilon) \right). \quad (4.1)$$

It is well known that in this case one should express the eigenvectors in terms of the matrix elements of the monodromy matrix:

$$L_\epsilon(v) = \left( R_{0,1}(v-u) R_{0,2}(v-\eta-\epsilon) \dots R_{0,2N-1}(v-u) R_{0,2N}(v-\eta-\epsilon) \times \right. \\ \left. \times \rho_0(q^{-1}) R_{0,2N+1}(v) R_{0,2N+2}(v-u+\eta-\epsilon) \dots R_{0,4N-1}(v) R_{0,4N}(v-u+\eta-\epsilon) \right) \quad (4.2)$$

$$L_\epsilon(v - \frac{\eta}{2}) = \begin{pmatrix} A_\epsilon(v) & B_\epsilon(v) \\ C_\epsilon(v) & D_\epsilon(v) \end{pmatrix}_0, \quad (4.3)$$

here, matrices  $A, B, C, D$  act in the Hilbert space of the spin chain, and  $M_\epsilon(v)$  is considered as a  $2 \times 2$  matrix in the auxiliary zero space.

The eigenvectors are given by a multiple product of  $B_\epsilon(x)$  operators acting on the pseudo vacuum  $|\uparrow \dots \uparrow\rangle$

$$|\mathbb{B}_\epsilon(x_1, \dots, x_n)\rangle = B_\epsilon(x_1) \dots B_\epsilon(x_n) |\uparrow \dots \uparrow\rangle. \quad (4.4)$$

The conditions for  $B_\epsilon(x_1, \dots, x_n)$  to be an eigenvector form the system of non-linear Bethe ansatz equations (BAE). It turns out that in our limit, the solution of the BAE is straightforward, and one gets nice formulas for the IM:

$$|Z\rangle = \frac{1}{(1+q^2)^{2N}} \left( \frac{\epsilon}{\sinh(\eta)} \right)^{N^2} |\mathbb{B}_\epsilon(\vec{x}_\epsilon)\rangle \Big|_{\epsilon \rightarrow 0}, \quad (4.5)$$



where the Bethe roots are given explicitly by:<sup>1</sup>

$$x_k = u + \frac{\epsilon}{1 - q^{\frac{1}{N}} e^{\frac{2i\pi}{N}(k-1/2)}}, \quad k \leq N \quad (4.6)$$

$$x_k = \frac{\epsilon}{1 - q^{\frac{1}{N}} e^{\frac{2i\pi}{N}(k-1/2)}}, \quad k > N \quad (4.7)$$

It is very rare that interacting integrable systems admit the exact and simple expressions for the Bethe roots; we point out the similarity of our formulas to the perimeter Bethe ansatz investigated by Baxter [24]. The price for this simplicity is, of course, the complicated limit  $\epsilon \rightarrow 0$  in Eq. (4.5). Despite this complication, Eqs. (4.5–4.7) lead to an exact expression for the IM in terms of multiple integrals. We hope to come back to these formulas in the future.

The same can be said about the dual IM:

$$\langle \mathcal{I} | = \frac{1}{(1 + q^2)^{2N}} \left( \frac{\epsilon}{\sin(\eta)} \right)^{N^2} \langle \mathbb{C}_\epsilon(\vec{x}_\epsilon) | \Big|_{\epsilon \rightarrow 0}. \quad (4.8)$$

Before analyzing the structure of the temporal transfer matrix and the influence matrix (IM) in detail, let us first compare our construction with the quantum transfer matrix (QTM) approach introduced by Sakai in [16] and further studied in [25, 26] in the context of the Loschmidt echo. The QTM formalism is specifically tailored for the thermodynamic limit, relying on a particular Trotterization of the evolution operator  $e^{itH}$ . Consequently, the QTM involves a regularization parameter  $\epsilon$ , which plays the role of a discrete Trotter step  $\delta t$ . For each finite  $\epsilon$ , the QTM spectrum remains non-degenerate, and the physical dynamics is recovered only in the scaling limit where the number of time steps tends to infinity and  $\epsilon \rightarrow 0$ .

In contrast, the influence matrix and the integrable transfer matrix introduced in this work are always physical, directly capturing the Floquet evolution of the integrable system. The cost of this physicality is that our transfer matrix is generically non-diagonalizable, unveiling novel and previously unexplored aspects of integrability.

In the following section, we explore these properties in detail by analyzing the free-fermionic limit of the model.

## 5 Free-fermionic point

We are interested in the long-time behavior of correlation functions; this demands the identification of long-range infrared degrees of freedom. To do so, let us first examine the free-fermionic point,  $\eta = \frac{\pi}{2}$ . In this case,  $\check{R}_{i,i+1}(v)$  turns into:

$$\check{R}_{i,i+1}(v) = e^{iJ_v(\sigma_i^+ \sigma_{i+1}^- + \sigma_i^- \sigma_{i+1}^+)}, \quad (5.1)$$

with  $J_v = \arcsin(-\tanh(v))$ .

After the Jordan-Wigner transformation:

$$c_i = \prod_{j<i} \sigma_j^z \sigma_i^-, \quad c_i^\dagger = \prod_{j<i} \sigma_j^z \sigma_i^+, \quad (5.2)$$

$$\{c_i, c_j\} = \{c_i^\dagger, c_j^\dagger\} = 0, \{c_i^\dagger, c_j\} = \delta_{i,j}, \quad (5.3)$$

$\check{R}$ -operator can be identified with a quadratic fermionic operator.

$$\check{R}_{i,i+1}(v) = e^{-iJ_v(c_i^\dagger c_{i+1} + c_{i+1}^\dagger c_i)}. \quad (5.4)$$

---

<sup>1</sup>In principle, these formulas have to be corrected with higher powers of  $\epsilon$ , as we have checked numerically, these solutions provide the exact IM up to  $4N = 16$  sites. We conjecture these formulas to be exact with no further corrections needed.

The resulting transfer matrix from the Eq. (3.8) has a Gaussian form, after the projection to a sector with fixed fermionic parity. Precisely, for  $q \neq 1$  we have that there are matrices  $Q^\pm$ , such that the transfer matrix takes the following form:

$$\begin{aligned} T(v) &= \frac{a(v)(q^2 - 1)}{q^2 + 1} \exp \left( \sum_{i,j=1}^{4N} Q_{i,j}^-(v) c_i^\dagger c_j \right), \text{ odd number of particles,} \\ T(v) &= a(v) \exp \left( \sum_{i,j=1}^{4N} Q_{i,j}^+(v) c_i^\dagger c_j \right), \text{ even number of particles,} \end{aligned} \quad (5.5)$$

where  $a(v)$  is the eigenvalue of the pseudovacuum:  $T(v)|\Omega\rangle = a(v)|\Omega\rangle$ ,  $a(v) = (\tanh(v) \tanh(u - v))^N$ .

Now, in the sector with fixed parity, the conjugation of single fermionic operators by a  $T(v)$  is given by:

$$T(v) c_i^\dagger T(v)^{-1} = \sum_{j=1}^{4N} M_{j,i}^\pm(v) c_j^\dagger, \quad (5.6)$$

where we introduced  $M^\pm = \exp(Q^\pm)$ , in the next section we describe matrices  $M^\pm$  in detail.

## 5.1 Local Integrals

Matrices  $M^\pm(v)$  commute for different values of  $v$ , but they are highly non-local, namely all matrix elements of  $M^\pm(v)$  are non-zero. In this section, we show the existence of local quadratic operators  $H_{l,r}^\pm$ , which still commute with  $M^\pm(v)$ . In order to describe the matrices  $H_{l,r}^\pm$ , it is convenient to use quantum and classical fermionic variables:

$$c_{i,cl}^{\pm,\dagger} = \frac{c_i^\dagger \mp q^2 c_{4N+1-i}^\dagger}{\sqrt{1 \pm q^2}}, \quad c_{i,cl}^\pm = \frac{c_i - c_{4N+1-i}}{\sqrt{1 \pm q^2}}, \quad (5.7)$$

$$c_{i,q}^{\pm,\dagger} = \frac{c_i^\dagger + c_{4N+1-i}^\dagger}{\sqrt{1 \pm q^2}}, \quad c_{i,q}^\pm = \frac{\pm q^2 c_i + c_{4N+1-i}}{\sqrt{1 \pm q^2}}. \quad (5.8)$$

It follows directly from the definition of the new fermions that the matrix  $M^\pm(v)$  does not mix them and can be presented as a direct sum  $M^\pm(v) = M^{\pm,cl}(v) \oplus M^{\pm,q}(v)$ . Even more importantly, the  $M^{\pm,cl/q}(v)$  entries become independent of  $q$  in this new basis and coincide in sectors of different parity.

Namely, the matrix  $M^{cl}(v)$  is lower-triangular, while  $M^q(v)$  is upper-triangular, and their entries are as follows:

$$\begin{aligned} M_{2i-1,2i-1}^{cl} &= -i \coth(u - v), \quad M_{2i,2i}^{cl} = i \tanh(v), \\ M_{2i-1+2k,2i-1}^{cl} &= -i \frac{\lambda_{cl}^{k-1}(v)}{\coth(v) \sinh^2(u - v)}, \quad M_{2i+2k,2i}^{cl} = -i \frac{\lambda_{cl}^{k-1}(v)}{\tanh(u - v) \cosh^2(v)}, \\ M_{i+2k-1,i}^{cl} &= -i \frac{\lambda_{cl}^{k-1}(v)}{\cosh(v) \sinh(u - v)}, \end{aligned} \quad (5.9)$$

$$\begin{aligned} M_{2i-1,2i-1}^q &= -i \tanh(u - v), \quad M_{2i,2i}^q = i \coth(v), \\ M_{2i-1,2i-1+2k}^q &= i \frac{\lambda_q^{k-1}(v)}{\tanh(v) \cosh^2(u - v)}, \quad M_{2i,2i+2k}^q = i \frac{\lambda_q^{k-1}(v)}{\coth(u - v) \sinh^2(v)}, \\ M_{i,i+2k-1}^q &= -i \frac{\lambda_q^{k-1}(v)}{\sinh(v) \cosh(u - v)}. \end{aligned} \quad (5.10)$$

here  $\lambda_{cl}(v) = \tanh(v) \coth(u - v)$ ,  $\lambda_q(v) = \tanh(u - v) \coth(v)$ .

In search of local integrals of motion (IOMs), let us introduce matrices  $h_l, h_r$ , which act locally:

$$(h_l^{cl})_{2i,2i} = 1, \quad (h_l^{cl})_{i+1,i} = -\frac{1}{\cosh(u)}, \quad (h_l^{cl})_{2i+1,2i-1} = 1. \quad (5.11)$$

$$(h_l^q)_{2i,2i} = 1, \quad (h_l^q)_{i,i+1} = \frac{1}{\cosh(u)}, \quad (h_l^q)_{2i-1,2i+1} = 1. \quad (5.12)$$

$$(h_r^{cl})_{2i-1,2i-1} = 1, \quad (h_r^{cl})_{i+1,i} = \frac{1}{\cosh(u)}, \quad (h_r^{cl})_{2i+2,2i} = 1. \quad (5.13)$$

$$(h_r^q)_{2i-1,2i-1} = 1, \quad (h_r^q)_{i,i+1} = -\frac{1}{\cosh(u)}, \quad (h_r^q)_{2i,2i+2} = 1, \quad (5.14)$$

and, according to the lemma below, commute with  $M(v)$ .

**Lemma 5.1.**  $[M^{cl/q}, h_{l/r}^{cl/q}] = 0$ .

*Proof.* Consider the matrix  $h_l^{cl}$ ; all other cases are analogous.

$$\begin{aligned} [M^{cl}, h_l^{cl}]_{2i+2k,2i} &= M_{2i+2k,2i}^{cl} - \frac{1}{\cosh(u)} M_{2i+2k,2i+1}^{cl} - M_{2i+2k,2i}^{cl} + \frac{1}{\cosh(u)} M_{2i+2k-1,2i}^{cl} = 0, \\ [M^{cl}, h_l^{cl}]_{2i+2k-1,2i-1} &= M_{2i+2k-1,2i+1}^{cl} - \frac{1}{\cosh(u)} M_{2i+2k+1,2i}^{cl} - M_{2i+2k-3,2i-1}^{cl} + \frac{1}{\cosh(u)} M_{2i+2k,2i-1}^{cl} = 0. \end{aligned}$$

The other case when the indices differ by an odd number requires more care. For example,

$$[M^{cl}, h_l^{cl}]_{2i+2k-2,2i-1} = M_{2i+2k-2,2i+1}^{cl} - \frac{1}{\cosh(u)} M_{2i+2k-2,2i}^{cl} - M_{2i+2k-2,2i-1}^{cl} + \frac{1}{\cosh(u)} M_{2i+2k-3,2i-1}^{cl}.$$

For  $k = 1$ , the first term vanishes, leaving:

$$\begin{aligned} [M^{cl}, h_l^{cl}]_{2i,2i-1} &= -\frac{i \tanh(v)}{\cosh(u)} + \frac{i}{\cosh(v) \sinh(u-v)} - \frac{i \coth(u-v)}{\cosh(u)} = \\ &= -i \frac{\sinh(v) \sinh(u-v) - \cosh(u) + \cosh(v) \cosh(u-v)}{\cosh(u) \cosh(v) \sinh(u-v)} = 0. \end{aligned}$$

For  $k > 1$ , all four terms contribute:

$$\begin{aligned} [M^{cl}, h_l^{cl}]_{2i+2k-2,2i-1} &= i \lambda_{cl}^{k-2} \left( -\frac{1}{\cosh(v) \sinh(u-v)} + \frac{1}{\cosh(u) \tanh(u-v) \cosh^2(u)} + \right. \\ &\quad \left. + \frac{\tanh(v) \coth(u-v)}{\cosh(v) \sinh(u-v)} - \frac{1}{\cosh(u) \coth(v) \sinh^2(u-v)} \right) = 0. \end{aligned}$$

The final equality  $[M^{cl}, h_l^{cl}]_{2i+2k-1,2i} = 0$  can be proved in the same manner.  $\square$

Using these matrices, one can define local and quadratic non-Hermitian ‘Hamiltonians’ which commute with the transfer matrix:

$$\begin{aligned}
H_l^{\pm,cl} &= \sum_{i=1}^N c_{2i,cl}^{\pm,\dagger} c_{2i,cl}^{\pm} - \sum_{i=1}^{2N-1} \frac{1}{\cosh(u)} c_{i+1,cl}^{\pm,\dagger} c_{i,cl}^{\pm} + \sum_{i=1}^N c_{2i+1,cl}^{\pm,\dagger} c_{2i-1,cl}^{\pm}, \\
H_l^{\pm,q} &= \sum_{i=1}^N c_{2i,q}^{\pm,\dagger} c_{2i,q}^{\pm} + \sum_{i=1}^{2N-1} \frac{1}{\cosh(u)} c_{i,q}^{\pm,\dagger} c_{i+1,q}^{\pm} + \sum_{i=1}^N c_{2i-1,q}^{\pm,\dagger} c_{2i+1,q}^{\pm}, \\
H_r^{\pm,cl} &= \sum_{i=1}^N c_{2i-1,cl}^{\pm,\dagger} c_{2i-1,cl}^{\pm} + \sum_{i=1}^{2N-1} \frac{1}{\cosh(u)} c_{i+1,cl}^{\pm,\dagger} c_{i,cl}^{\pm} + \sum_{i=1}^N c_{2i+2,cl}^{\pm,\dagger} c_{2i,cl}^{\pm}, \\
H_r^{\pm,q} &= \sum_{i=1}^N c_{2i-1,q}^{\pm,\dagger} c_{2i-1,q}^{\pm} - \sum_{i=1}^{2N-1} \frac{1}{\cosh(u)} c_{i,q}^{\pm,\dagger} c_{i+1,q}^{\pm} + \sum_{i=1}^N c_{2i,q}^{\pm,\dagger} c_{2i+2,q}^{\pm}.
\end{aligned} \tag{5.15}$$

These Hamiltonians are closely related to those obtained in [27,28] for alternating spin chains. However, we were unable to identify local Hamiltonians commuting with the transfer matrix outside the free fermionic point. The standard approach to constructing local integrals of motion — via the logarithmic derivative of the transfer matrix evaluated at the inhomogeneity points,  $H_\alpha^{\text{loc}} = T(v_\alpha)^{-1} T'(v_\alpha)$ , with  $v_\alpha \in 0, u, i\eta, u + i\eta$  — breaks down in our case, as  $T(v_\alpha)$  is not invertible.

In the next section, we study the Jordan block structure of these Hamiltonians. As we will explain, they share the same Jordan blocks with the transfer matrix.

Due to the fact that the transfer matrix preserves fermionic parity, and the IM is a state with an even number of fermions, we restrict ourselves to this sector only, omitting the indices  $\pm$ .

## 5.2 Combinatorics of Jordan blocks

In the previous section, we introduced the action  $M(v) = M^{\text{cl}}(v) \oplus M^q(v)$  of the transfer matrix on the single-particle sector, and the local Hamiltonian  $h_{l/r} = h_{l/r}^{\text{cl}} \oplus h_{l/r}^q$ , commuting with  $M(v)$ .

The goal of the current section is to study the Jordan decomposition of the single-particle matrix  $M(v)$  and its extension to the full many-body operator  $T(v)$ . Let us start with a Jordan decomposition of a single-particle operator:

**Lemma 5.2.** *The canonical form of the matrices  $h_{l/r}^{\text{cl}/q}$  and  $M^{\text{cl}/q}$  comprises exactly two Jordan blocks, each with a size of  $N$ .*

*Proof.* We first notice that all given matrices are upper or lower triangular, so the entries on their diagonals are exactly the eigenvalues counted with the algebraic multiplicity. In particular, all matrices have only two distinct eigenvalues, both repeated  $N$  times, which correspond to the dimension of an associated root subspace. Then, to finish the proof, it suffices to show that the geometric multiplicity of each eigenvalue is 1, i.e., there is a unique eigenvector up to scale. This fact can be checked directly.  $\square$

**Lemma 5.3.** *Matrices  $h_{l/r}^{\text{cl}/q}$  and  $M^{\text{cl}/q}$  share common simple root subspaces of dimension  $N$ .*

*Proof.* The preceding lemma guarantees that root subspaces of all matrices are simple and have dimension  $N$ . Then, from the commutativity of  $h_{l/r}$  and  $M$ , it follows that  $M^{\text{cl}/q}$  acts invariantly on root subspaces of  $h_{l/r}^{\text{cl}/q}$ . Finally, because the dimensions of the root subspaces coincide, the statement of this lemma holds.  $\square$

As we now perfectly understand the structure of the single-particle Jordan decomposition, we are ready to lift it to the many-particle sector. As we will see below, it turns out to be a non-trivial mathematical question. Luckily, the problem was partially addressed in [18], where the authors fully described the Jordan block structure of the

quadratic Hamiltonian  $H_k = \sum_{i=1}^{M-1} \psi_i^\dagger \psi_{i-1}$ . We review their results below. For now, let us outline our strategy for obtaining the Jordan block structure in our case. As a first step, we identify what we call the canonical form of the operator  $T(v)$ . Then, using the results of [18] and one additional lemma, we derive the formula (5.27) for the number of Jordan blocks of a given size  $d$ . After that, we numerically analyze this formula, showing that the number of Jordan blocks of a given size grows exponentially with the number of time steps  $2N$ .

Let us proceed with the canonical forms: as stated before, in the sector with even parity  $T(v)$  takes the Gaussian form:  $T(v) = a(v) e^{\sum_{i,j=1}^{4N} (\log M)_{i,j} c_i^\dagger c_j}$ , with  $a(v) = (\tanh(v) \tanh(u-v))^N$ .

In this section, we are interested in the Jordan canonical form only, and identify operators related by a similarity transformation  $A \sim B$ , if  $A = OBO^{-1}$  for some invertible  $O$ . We note, the matrices  $M$  and  $f(M)$  are similar  $M \sim f(M)$  and have the same Jordan canonical structure, as long as  $f$  is analytic at points  $\lambda_i$  corresponding to the eigenvalues of  $M$ .

Let us now introduce a new set of fermions that bring  $\log(M)$  into its canonical form:

$$\psi_i^\dagger = \sum_{j=1}^{4N} A_{j,i} c_j^\dagger, \quad \psi_i = \sum_{j=1}^{4N} A_{i,j}^{-1} c_j, \quad (5.16)$$

where  $A$  is an arbitrary matrix, such that  $A^{-1} \log(M) A$  takes the transpose canonical Jordan form of a matrix  $\log(M)$ . Recalling that  $M$  and  $\log(M)$  have four different Jordan blocks, we denote  $\psi_{\alpha,i}$  with  $\alpha = 1, \dots, 4$  and  $i = 1 \dots N$  the span of each of these blocks. The transfer matrix takes the form:

$$T(v) = a(v) \prod_{\alpha=1}^4 e^{\log(\Lambda_\alpha) \sum_{k=1}^N \psi_{\alpha,k}^\dagger \psi_{\alpha,k} + \sum_{k=1}^{N-1} \psi_{\alpha,k+1}^\dagger \psi_{\alpha,k}} \sim a(v) e^{\sum_{\alpha=1}^4 \log(\Lambda_\alpha) \sum_{k=1}^N \psi_{\alpha,k}^\dagger \psi_{\alpha,k}} \left(1 + \sum_{\alpha=1}^4 \sum_{k=1}^{N-1} \psi_{\alpha,k+1}^\dagger \psi_{\alpha,k}\right). \quad (5.17)$$

We call such an expression a canonical form of the transfer matrix. We see that, up to a diagonal contribution  $\sum_{k=1}^N \psi_{\alpha,k}^\dagger \psi_{\alpha,k}$ , it is a sum of four canonical Hamiltonians  $H_\alpha$ :

$$H_\alpha = \sum_{k=1}^{N-1} \psi_{\alpha,k+1}^\dagger \psi_{\alpha,k}. \quad (5.18)$$

As mentioned above, the calculation of Jordan blocks of such quadratic fermionic forms was carefully studied in [18]. Let us describe their results here. Corollary 3.4 of [18] states that for the nilpotent operator  $H_\alpha$ , restricted to a sector with  $n$  particles, the number of Jordan blocks of a given size  $d$  is given by the difference:

$$\mathcal{N}_n^d = V_{N,n}^{\lfloor \frac{n(N-n)}{2} - \frac{d-1}{2} \rfloor} - V_{N,n}^{\lfloor \frac{n(N-n)}{2} - \frac{d+1}{2} \rfloor}, \quad n(N-n) - d : \text{ odd} \quad (5.19)$$

$$\mathcal{N}_n^d = 0, \quad n(N-n) - d : \text{ even} \quad (5.20)$$

The numbers  $V_{M,n}^{[r]}$  are given in terms of the q-binomial coefficients:

$$\begin{bmatrix} M \\ n \end{bmatrix}_q = \frac{[M]_q!}{[M-n]_q! [n]_q!} = \sum_{r=0}^{n(M-n)} q^r V_{M,n}^{[r]}, \quad (5.21)$$

here  $[n]_q = \frac{1-q^n}{1-q}$ ,  $[n]_q! = \prod_{k=1}^n [k]_q$ .

Making use of the corollary, we first decompose each of the Hamiltonians  $H_\alpha$  into a direct sum of Jordan blocks for the fixed number of particles  $n_\alpha$ :

$$H_\alpha \sim \bigoplus_{d_\alpha, 1 \leq i_{d_\alpha} \leq \mathcal{N}_{n_\alpha}^{d_\alpha}} \mathcal{H}_{\alpha, d_\alpha, i_{d_\alpha}}, \quad (5.22)$$

where each  $\mathcal{H}_{\alpha, d_\alpha, i_{d_\alpha}}$  is a single canonical Jordan cell with eigenvalue 0 and size  $d_\alpha$ , different Jordan cells of the same size  $d_\alpha$  are enumerated by the index  $i_{d_\alpha}$ . Thus, we obtain the following decomposition of the transfer matrix:

$$T(v) \sim a(v) \bigoplus_{n_\alpha, d_\alpha, i_{d_\alpha}} (\Lambda^{\vec{n}} I + \sum_{\alpha=1}^4 \mathcal{H}_{\alpha, d_\alpha, i_{d_\alpha}}), \quad (5.23)$$

here  $n_\alpha$  is the number of particles in each sector  $\alpha$ , and  $\Lambda^{\vec{n}} = \prod_{i=1}^4 \Lambda_i^{n_i}$ . We assume that we initially have a fixed number of particles in classical and quantum sectors:  $n_{cl} = n_q = n_1 + n_2 = n_3 + n_4 = N$ . However, if we concentrate on a fixed eigenvalue as well, this will uniquely fix all four  $n_\alpha$ . Despite the fact that each of the operators  $\mathcal{H}_{\alpha, d_\alpha, i_{d_\alpha}}$  is in a Jordan canonical form, the sum of the four admits further decomposition. To perform this decomposition, we note the analogy between  $\mathcal{H}_{\alpha, d_\alpha, i_{d_\alpha}}$  operators and spin operators  $S_{\alpha, d_\alpha}^+$ , where  $S_{\alpha, d_\alpha}^+$  is a part of an  $SU(2)$  triplet:

$$S_{\alpha, d_\alpha}^+, S_{\alpha, d_\alpha}^-, S_{\alpha, d_\alpha}^z, \quad (5.24)$$

in a representation of dimension  $d_\alpha$ . As a result, the following lemma is obtained:

**Lemma 5.4.** *The sum of Jordan canonical matrices  $\sum_{\alpha=1}^4 \mathcal{H}_{\alpha, d_\alpha, i_{d_\alpha}}$  admits the following decomposition:*

$$\sum_{\alpha=1}^4 \mathcal{H}_{\alpha, d_\alpha, i_{d_\alpha}} \sim \bigoplus_{D=1}^{\sum_{\alpha=1}^4 d_\alpha - 3} \bigoplus_{k=1}^{C_d^D} J_{D, k, \vec{i}_{d_\alpha}}, \quad (5.25)$$

where  $J_{D, k, \vec{i}_{d_\alpha}}$  is a Jordan cell of size  $D$  and  $C_d^D$  denotes multiplicities, given by the formula:

$$C_d^D = \frac{1}{\pi} \int_0^{2\pi} \frac{\sin(D\phi) \prod_{\alpha} \sin(d_\alpha \phi)}{(\sin(\phi))^3} d\phi. \quad (5.26)$$

In particular,  $C_d^D = 0$  if  $D - \sum_{\alpha} d_\alpha$  is even.

*Proof.* From the representation theory, it is known that the character of the irreducible representation of  $SU(2)$  of dimension  $d$  is given by the formula  $\chi_d(\phi) = \frac{\sin(d\phi)}{\sin(\phi)}$ . Then, the multiplicity of the representation with dimension  $D$  can be computed as the scalar product of characters:

$$C_d^D = \langle \chi_D | \prod_{\alpha} \chi_{d_\alpha} \rangle = \frac{2}{\pi} \int_0^\pi \frac{\sin(D\phi) \prod_{\alpha} \sin(d_\alpha \phi)}{(\sin(\phi))^5} (\sin(\phi))^2 d\phi.$$

In addition, it is known that the parity of dimension  $D$  should coincide with the parity of  $\sum_{\alpha} d_\alpha - 1$ . Otherwise, the multiplicity is zero.  $\square$

This lemma finishes the decomposition of  $T(v)$  into Jordan blocks. The final multiplicities of a Jordan block of size  $D$  in the sector with fixed occupation numbers  $n_\alpha$  are given by the sum:

$$\text{Mult}_{N,\vec{n}}^D = \sum_{d_\alpha} C_{\vec{d}}^D \mathcal{N}_{\vec{n}}^{\vec{d}}, \quad (5.27)$$

where  $\mathcal{N}_{\vec{n}}^{\vec{d}} = \prod_{\alpha=1}^4 \mathcal{N}_{n_\alpha}^{d_\alpha}$ .

As we explain in the appendix (B), Eq. (5.27) can be rewritten as a difference of two integrals:

$$\text{Mult}_{N,\vec{n}}^D = V_{N,\vec{n}}^{+,D} - V_{N,\vec{n}}^{-,D}, \quad (5.28)$$

where the numbers  $V_{N,\vec{n}}^{\pm,D}$  are given by the following formula:

$$V_{N,\vec{n}}^{\pm,D} = \frac{1}{2\pi i} \oint \left[ \begin{matrix} N \\ n_1 \end{matrix} \right]_q \cdots \left[ \begin{matrix} N \\ n_4 \end{matrix} \right]_q q^{-\frac{\sum_\alpha n_\alpha (N - n_\alpha) + D \mp 1}{2}} dq. \quad (5.29)$$

In the same appendix, we argue that these integrals can be efficiently estimated by the saddle point method, with the saddle point value  $q^* = e^{\frac{2\pi x^*}{N+1}}$  being close to 1:

$$x_\pm^* = \frac{3(D \mp 1)}{\pi \sum_\alpha n_\alpha (N - n_\alpha)}. \quad (5.30)$$

Substituting the saddle point into Eq. (5.28) we obtain the approximate formula for multiplicities:

$$\text{Mult}_{N,\vec{n}}^D \approx \prod_\alpha \binom{N}{n_\alpha} \left( \frac{1}{6} \pi^{1/3} \sum_\alpha n_\alpha (N - n_\alpha) (N + 1) \right)^{-3/2} D \exp \left( - \frac{3D^2}{2 \sum_\alpha n_\alpha (N - n_\alpha) (N + 1)} \right). \quad (5.31)$$

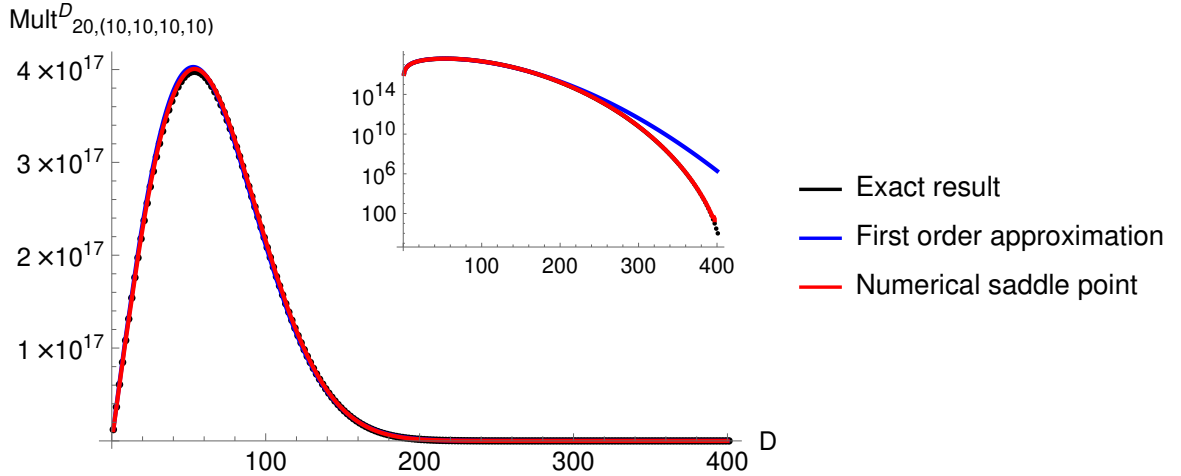


Figure 6: Comparison between the exact values of the multiplicity  $\text{Mult}_{N,\vec{n}}^D$  and their approximation from the steepest descent method. The blue line is drawn according to Eq. (5.31), while the red line is obtained by solving the saddle point equation numerically and substituting in into the exact  $q$ -binomial coefficients ( $N = 20, n_1 = \cdots = n_4 = 10$ ).

The distribution of Jordan blocks remains the same for all  $v \neq 0, u$ . In the latter case, the inverse of the transfer matrix from (5.6) is not well-defined, and our methods cannot be applied to find the degeneracy.

### 5.3 Basis of short-ranged wave functions

In this section, we further analyze the spatial structure of Jordan blocks in order to reveal the entanglement structure of the IM.

As was explained in section 2, the IM is a unique eigenstate of the transfer matrix with eigenvalue 1. In the single-particle sector, the transfer matrix has four different Jordan blocks. Let us denote the corresponding wave functions that span each of the four Jordan blocks as  $\Psi_{cl/q,\alpha,i}^\dagger$ :

$$\Psi_{cl/q,\alpha,i}^\dagger = \sum_{k=1}^{2N} c_{k,cl/q}^\dagger J_{i,k}^{\alpha,cl/q}, \quad (5.32)$$

where  $\alpha = 0, 1$  indicates a Jordan block with the eigenvalue  $\alpha$ , and the labels cl/q indicate the classical/quantum sectors introduced in Eq. (5.7). The IM can be created by fully occupying two of the four possible Jordan blocks using the creation operators  $\Psi_{q,1,i}^\dagger, \Psi_{cl,0,i}^\dagger$  acting on the reference vacuum state  $|\Omega\rangle$ :

$$|\mathcal{I}\rangle \propto \prod_{i=1}^N \Psi_{q,1,i}^\dagger \Psi_{cl,0,i}^\dagger |\Omega\rangle. \quad (5.33)$$

Indeed, it can be seen from Eq. (3.12) that  $T(v)|\Omega\rangle = a(v)|\Omega\rangle = (\tanh(v) \tanh(u-v))^N |\Omega\rangle$ , and therefore:

$$T(v)|\mathcal{I}\rangle \propto \prod_{i=1}^N T(v) \Psi_{q,1,i}^\dagger T(v)^{-1} T(v) \Psi_{cl,0,i}^\dagger T(v)^{-1} T(v) |\Omega\rangle = (\Lambda_{cl,0} \Lambda_{q,1} \tanh(v) \tanh(u-v))^N |\mathcal{I}\rangle = |\mathcal{I}\rangle. \quad (5.34)$$

The normalization in Eq. (5.33) can be fixed by imposing the trace property defined by Eq. (2.6). By fixing the normalization of the wave functions as:

$$\hat{J}_{N,2N-1}^{0,cl} = \hat{J}_{1,2}^{1,q} = 1, \quad \hat{J}_{i+1,k+2}^{0,cl} = \hat{J}_{i,k}^{0,cl}, \quad \hat{J}_{i+1,k+2}^{1,q} = \hat{J}_{i,k}^{1,q} \quad (5.35)$$

and requiring  $|J_1^{0,cl}\rangle, |J_N^{1,q}\rangle$  to be the highest vectors, we obtain the trivial proportionality constant:

$$|\mathcal{I}\rangle = \prod_{i=1}^N \Psi_{q,1,i}^\dagger \Psi_{cl,0,i}^\dagger |\Omega\rangle, \quad (5.36)$$

where the derivation is given in appendix C.

In order to investigate the entanglement properties of the IM, note that the Eq. (5.36) remains invariant (up to a proportionality constant) under basis transformations inside of the linear envelope of each of the Jordan blocks:

$$J_{i,k}^{\alpha,cl,q} \rightarrow \sum_{j=1}^N C_{i,j} J_{j,k}^{\alpha,cl/q}, \quad (5.37)$$

for some non-degenerate matrix  $C_{i,j}$ .

In the appendix C.1, we introduce explicitly a basis in each of the Jordan blocks, which is suitable for practical computations. In particular, we provide a numerical routine for the computation of the orthogonal basis, such that the components of the wave functions obey the causality property in the sense that  $i$ -th wave function is supported on the first (last)  $2i$  time sites, and has polynomially decaying tails:

$$\begin{aligned} \hat{J}_{1,2k-1}^{0,cl} &= \hat{J}_{N,2N-2k+2}^{1,q} \approx \frac{A_1}{k^{3/2}} \sin(\omega(s)k - \phi_1) + \frac{B_1}{k^{3/2}(N-k+1)} \sin(\omega(s)k - \Phi_1), \quad k \gg 1 \\ \hat{J}_{1,2k}^{0,cl} &= \hat{J}_{N,2N-2k+1}^{1,q} \approx \frac{A_2}{k^{3/2}} \sin(\omega(s)k - \phi_2) + \frac{B_2}{k^{3/2}(N-k+1)} \sin(\omega(s)k - \Phi_2), \quad k \gg 1 \end{aligned} \quad (5.38)$$



where  $\omega(s) = 2 \arcsin(s)$  and the vectors are normalized so that  $\hat{j}_{m,2m-1}^{0,cl} = \hat{j}_{m,2m}^{1,q} = 1$ .

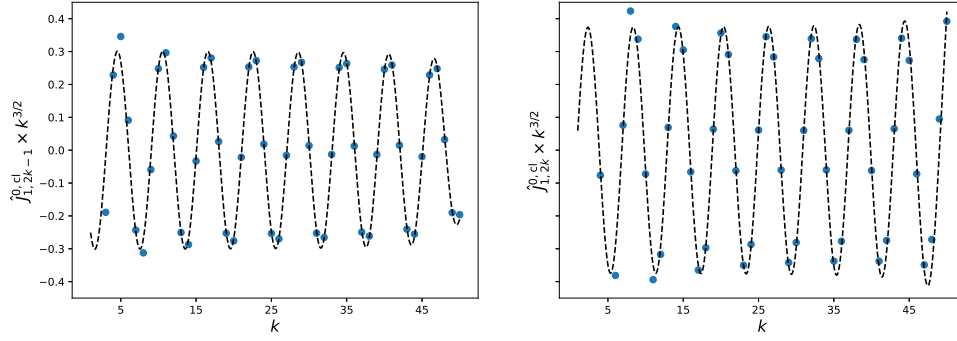


Figure 7: Components of the highest vector in the orthogonal basis for  $N = 50$ ,  $s = \frac{1}{2}$ . The fitting constants are shown below:

$A_1$	$A_2$	$B_1$	$B_2$	$\phi_1$	$\phi_2$	$\Phi_1$	$\Phi_2$
0.303	0.371	0.138	0.210	3.083	-0.880	-0.589	1.735

This guarantees the existence of a quasi-local gapped Hamiltonian in agreement with a similar observation for the kicked Ising model [12].

## 6 Conclusion

In this article, we investigated the IM approach to the integrable Floquet dynamics. We revealed an interesting integrable structure rooted in the non-diagonalizable transfer matrix. We have conjectured an exact expression for the IM as a Bethe vector provided by Eq. (4.5) with exact Bethe roots given by Eqs. (4.6–4.7).

**Relation to QTM approach** Our construction is similar in spirit to the so-called QTM approach introduced by Sakai in [16]. While Sakai’s approach works only in the continuous limit, our construction can be applied to a discretized Floquet system. This difference leads to a different organization of Bethe roots and results in novel non-diagonalizable integrable transfer matrices.

**Free-fermionic limit to XX chain** We also studied in detail the free-fermionic limit to the XX chain. In this case, we identified an interesting family of local Hamiltonians, commuting with the temporal transfer matrix provided by the Eqs. (5.15).

We also managed to study the distribution of Jordan blocks given by the approximate Eq. (5.31). This equation predicts the exponentially many blocks of thermodynamically large size, qualitatively explaining the temporal entanglement barrier effect reported earlier [12, 20].

Finally, we examined the structure of the single-particle wave functions related to each of the Jordan blocks. We found that though the canonical Jordan basis leads to the unnormalizable wave functions, each invariant subspace can be spanned by the wave functions with a polynomial decay.

**Future directions: IM approximation and correlation functions** The polynomially decaying basis can be used to construct a matrix product state (MPS) approximation of the IM, for example, using the technique in [29]. This approximation would provide a non-trivial tool to study the dynamics of an integrability-breaking impurity at the boundary of the free-fermionic model [30]. It is therefore natural to seek an interacting counterpart by

studying perturbations away from free fermions. We expect this perturbation theory to be stable, as suggested by the logarithmic growth of the temporal entanglement of the IM in the XXZ spin chain reported in [13]. We plan to pursue this direction further and to develop an efficient tool for computing dynamical correlation functions in the XXZ model with broken integrability.

## 7 Acknowledgments

We are grateful to Balázs Pozsgay for his comments on a later version of this article. We also thank Alessio Lerose and Dmitry Abanin for their interest in the work and their support during its early stages. I.V. further thanks Žiga Krajnik for discussions on the IM approach to integrable systems, and Heran Wang for numerical calculations relevant to this work, which are not included in the present article.

## References

- [1] J.-S. Caux, R. Hagemans and J. M. Maillet, *Computation of dynamical correlation functions of heisenberg chains: the gapless anisotropic regime*, Journal of Statistical Mechanics: Theory and Experiment **2005**(09), P09003 (2005).
- [2] N. Kitanine, J. Maillet, N. Slavnov and V. Terras, *On the algebraic bethe ansatz approach to the correlation functions of the xxz spin-1/2 heisenberg chain*, arXiv preprint hep-th/0505006 (2005).
- [3] C. Babenko, F. Göhmann, K. K. Kozłowski, J. Sirker and J. Suzuki, *Exact real-time longitudinal correlation functions of the massive xxz chain*, Physical Review Letters **126**(21), 210602 (2021).
- [4] O. A. Castro-Alvaredo, B. Doyon and T. Yoshimura, *Emergent hydrodynamics in integrable quantum systems out of equilibrium*, Physical Review X **6**(4), 041065 (2016), doi:10.1103/PhysRevX.6.041065.
- [5] B. Bertini, M. Collura, J. De Nardis and M. Fagotti, *Transport in out-of-equilibrium xxz chains: exact profiles of charges and currents*, Physical review letters **117**(20), 207201 (2016), doi:10.1103/PhysRevLett.117.207201.
- [6] M. Ljubotina, M. Žnidarič and T. c. v. Prosen, *Kardar-parisi-zhang physics in the quantum heisenberg magnet*, Phys. Rev. Lett. **122**, 210602 (2019), doi:10.1103/PhysRevLett.122.210602.
- [7] Ž. Krajnik and T. Prosen, *Kardar-parisi-zhang physics in integrable rotationally symmetric dynamics on discrete space-time lattice*, Journal of Statistical Physics **179**(1), 110 (2020), doi:10.1007/s10955-020-02523-1.
- [8] C. Destri and H. De Vega, *Light-cone lattice approach to fermionic theories in 2d: The massive thirring model*, Nuclear Physics B **290**, 363 (1987), doi:10.1016/0550-3213(87)90193-3.
- [9] C. Destri and T. Segalini, *A local and integrable lattice regularization of the massive thirring model*, Nuclear Physics B **455**(3), 759 (1995), doi:10.1016/0550-3213(95)00496-F.
- [10] M. Vanicat, L. Zadnik and T. Prosen, *Integrable trotterization: Local conservation laws and boundary driving*, Physical review letters **121**(3), 030606 (2018), doi:10.1103/PhysRevLett.121.030606.
- [11] Y. Miao, V. Gritsev and D. V. Kurlov, *The floquet Baxterisation*, SciPost Physics **16**(3), 078 (2024), doi:10.21468/SciPostPhys.16.3.078.
- [12] A. Lerose, M. Sonner and D. A. Abanin, *Influence matrix approach to many-body floquet dynamics*, Physical Review X **11**(2), 021040 (2021), doi:10.1103/PhysRevX.11.021040.

- [13] G. Giudice, G. Giudici, M. Sonner, J. Thoenniss, A. Lerose, D. A. Abanin and L. Piroli, *Temporal entanglement, quasiparticles, and the role of interactions*, Physical review letters **128**(22), 220401 (2022), doi:10.1103/PhysRevLett.128.220401.
- [14] P. W. Claeys, J. Herzog-Arbeitman and A. Lamacraft, *Correlations and commuting transfer matrices in integrable unitary circuits*, SciPost Physics **12**(1), 007 (2022), doi:10.21468/SciPostPhys.12.1.007.
- [15] F. Göhmann, A. Klümper and A. Seel, *Integral representations for correlation functions of the xxz chain at finite temperature*, Journal of Physics A: Mathematical and General **37**(31), 7625 (2004).
- [16] K. Sakai, *Dynamical correlation functions of the xxz model at finite temperature*, Journal of Physics A: Mathematical and Theoretical **40**(27), 7523 (2007), doi:10.1088/1751-8113/40/27/007.
- [17] T. Prosen, *Spectral theorem for the lindblad equation for quadratic open fermionic systems*, Journal of Statistical Mechanics: Theory and Experiment **2010**(07), P07020 (2010), doi:10.1088/1742-5468/2010/07/P07020.
- [18] S. Kitahama, H. Yoshida, R. Toyota and H. Katsura, *Jordan decomposition of non-hermitian fermionic quadratic forms*, Journal of Statistical Mechanics: Theory and Experiment **2024**(1), 013101 (2024), doi:10.1088/1742-5468/ad0f98.
- [19] A. Lerose, M. Sonner and D. A. Abanin, *Overcoming the entanglement barrier in quantum many-body dynamics via space-time duality*, Physical Review B **107**(6), L060305 (2023), doi:10.1103/PhysRevB.107.L060305.
- [20] J. Yao and P. W. Claeys, *Temporal entanglement barriers in dual-unitary clifford circuits with measurements*, Physical Review Research **6**(4), 043077 (2024), doi:10.1103/PhysRevResearch.6.043077.
- [21] A. Lerose, M. Sonner and D. A. Abanin, *Scaling of temporal entanglement in proximity to integrability*, Phys. Rev. B **104**, 035137 (2021), doi:10.1103/PhysRevB.104.035137.
- [22] M. Ljubotina, M. Žnidarič and T. Prosen, *Spin diffusion from an inhomogeneous quench in an integrable system*, Nature communications **8**(1), 16117 (2017), doi:10.1038/ncomms16117.
- [23] V. B. Bulchandani, R. Vasseur, C. Karrasch and J. E. Moore, *Bethe-boltzmann hydrodynamics and spin transport in the xxz chain*, Physical review B **97**(4), 045407 (2018), doi:10.1103/PhysRevB.97.045407.
- [24] R. J. Baxter, *Perimeter bethe ansatz*, Journal of Physics A: Mathematical and General **20**(9), 2557 (1987), doi:10.1088/0305-4470/20/9/039.
- [25] B. Pozsgay, *The dynamical free energy and the loschmidt echo for a class of quantum quenches in the heisenberg spin chain*, Journal of Statistical Mechanics: Theory and Experiment **2013**(10), P10028 (2013), doi:10.1088/1742-5468/2013/10/P10028.
- [26] L. Piroli, B. Pozsgay and E. Vernier, *What is an integrable quench?*, Nuclear Physics B **925**, 362 (2017), doi:10.1016/j.nuclphysb.2017.10.012.
- [27] Y. Ikhlef, J. Jacobsen and H. Saleur, *A staggered six-vertex model with non-compact continuum limit*, Nuclear Physics B **789**(3), 483 (2008), doi:10.1016/j.nuclphysb.2007.07.004.
- [28] V. V. Bazhanov, G. A. Kotousov, S. M. Koval and S. L. Lukyanov, *Scaling limit of the z2 invariant inhomogeneous six-vertex model*, Nuclear Physics B **965**, 115337 (2021), doi:10.1016/j.nuclphysb.2021.115337.
- [29] M. T. Fishman and S. R. White, *Compression of correlation matrices and an efficient method for forming matrix product states of fermionic gaussian states*, Physical Review B **92**(7), 075132 (2015).

- [30] J. Thoenniss, M. Sonner, A. Leroze and D. A. Abanin, *Efficient method for quantum impurity problems out of equilibrium*, Physical Review B **107**(20), L201115 (2023).
- [31] S. Banerjee and B. Wilkerson, *Lambert series and  $q$ -functions near  $q=1$* , International Journal of Number Theory **13**(08), 2097 (2017), doi:10.1142/S1793042117501135.
- [32] B. Parisse and M. Vaughan, *Jordan normal and rational normal form algorithms*, arXiv.org (2004), doi:10.48550/arXiv.cs/0412005.
- [33] J. I. Rubiano-Murcia and J. Galvis, *Higher order derivatives of the adjugate matrix and the jordan form*, Linear Algebra and its Applications **680**, 137 (2024), doi:10.1016/j.laa.2023.10.005.

## A Bethe ansatz equations

The spectrum of the deformed transfer matrix (4.1) can be found by solving the BAE equations:

$$\left( \frac{\sinh(x_i - u - \eta)}{\sinh(x_i - u)} \frac{\sinh(x_i - \eta)}{\sinh(x_i)} \frac{\sinh(x_i + \epsilon)}{\sinh(x_i + \epsilon + \eta)} \frac{\sinh(x_i - u + \epsilon)}{\sinh(x_i - u + \eta + \epsilon)} \right)^N = -q^{-2} \prod_{j \neq i} \frac{\sinh(x_i - x_j + \eta)}{\sinh(x_i - x_j - \eta)}. \quad (\text{A.1})$$

We see that formally, in the limit  $\epsilon \rightarrow 0$  a number of cancellations occur, which reduces the number of solutions. This means that this limit should be taken more carefully. Let us rewrite the left-hand side of Eq. (A.1):

$$\left( \frac{\sinh(x_i - u + \epsilon)}{\sinh(x_i - u)} \frac{\sinh(x_i + \epsilon)}{\sinh(x_i)} \frac{\sinh(x_i - \eta)}{\sinh(x_i + \eta)} \frac{\sinh(x_i - u - \eta)}{\sinh(x_i - u + \eta)} \right)^N = -q^{-2} \prod_{j \neq i} \frac{\sinh(x_i - x_j + \eta)}{\sinh(x_i - x_j - \eta)}, \quad (\text{A.2})$$

where we have omitted  $\epsilon$  whenever it does not lead to a cancellation. Now if we compare this to the BAE for a spin chain on  $N$  sites with  $n$  magnons, arbitrary evaluation parameters  $v_a$  and spins  $s_a \in \mathbb{Z}/2$  at each site:

$$\prod_{a=1}^{2N} \frac{\sinh(x_i - v_a - s_a \eta)}{\sinh(x_i - v_a + s_a \eta)} = -q^2 \prod_{j \neq i} \frac{\sinh(x_i - x_j + \eta)}{\sinh(x_i - x_j - \eta)}, \quad (\text{A.3})$$

we can identify that:

- The source terms  $\left( \frac{\sinh(x_i - u - \eta)}{\sinh(x_i - u + \eta)} \right), \left( \frac{\sinh(x_i - \eta)}{\sinh(x_i + \eta)} \right)$  correspond to spin-one sites.
- the source terms  $\left( \frac{\sinh(x_i - u + \epsilon)}{\sinh(x_i - u)} \right), \left( \frac{\sinh(x_i + \epsilon)}{\sinh(x_i)} \right)$  are the functions which equal to 1 everywhere except the vicinity of the points  $x_0^+ = u, x_0^- = 0$  respectively.

Now it is straightforward to classify the solutions of Eqs. (A.2). First, we assume that all Bethe roots are away from the resonance points  $x_k \neq u, 0$ . In this case, we may neglect the last two multipliers, ending up with a spin-one chain on  $2N$  sites, which provides us with  $3^{2N}$  solutions. Now we can place some of the Bethe roots at the resonance points:

$$x_k = u + \epsilon \chi_k, \quad \text{for } k \leq k_+ \quad (\text{A.4})$$

$$x_k = \epsilon \chi_k, \quad \text{for } k^+ < k \leq k_+ + k_- \quad (\text{A.5})$$

$$x_k - \text{are away from the resonance points}, \quad \text{for } k > k_+ + k_- \quad (\text{A.6})$$

In this case, Bethe equations split into three systems of equations:

$$\left( \frac{\chi_k - 1}{\chi_k} \right)^N \left( \frac{\sinh(x_k - u - \eta)}{\sinh(x_k - u + \eta)} \right)^{N - k_-} (-1)^{N - k_+} = -q^{-2} \prod_{j=k_+ + k_- + 1}^{2N} \frac{\sinh(u - x_j + \eta)}{\sinh(u - x_j - \eta)}, \quad \text{for } k \leq k_+ \quad (\text{A.7})$$

$$\left( \frac{\chi_k - 1}{\chi_k} \right)^N \left( \frac{\sinh(x_k - \eta)}{\sinh(x_k + \eta)} \right)^{N - k_+} (-1)^{N - k_-} = -q^{-2} \prod_{j=k_+ + k_- + 1}^{2N} \frac{\sinh(x_j - \eta)}{\sinh(x_j + \eta)}, \quad \text{for } k^+ < k \leq k_+ + k_- \quad (\text{A.8})$$

$$\left( \frac{\sinh(x_k - u - \eta)}{\sinh(x_k - u + \eta)} \right)^{N - k_+} \left( \frac{\sinh(x_k - \eta)}{\sinh(x_k + \eta)} \right)^{N - k_-} = -q^{-2} \prod_{j=k_+ + k_- + 1}^{2N} \frac{\sinh(x_k - x_j + \eta)}{\sinh(x_k - x_j - \eta)}, \quad \text{for } k > k_+ + k_- \quad (\text{A.9})$$

The third equation is nothing but the BAE for a spin-one chain on  $2N - k_+ - k_-$  sites with  $2N - k_+ - k_-$  magnons. If one could solve these equations (for e.g. numerically), then the first two equations could be easily solved analytically. Note that in the limit  $\epsilon \rightarrow 0$  Bethe roots merge together, which produces a degenerate subspace for the transfer matrix and Jordan blocks. The IM itself is the leading eigenvector with the highest eigenvalue 1 corresponding to the case of  $k_+ = k_- = N$ , in which case one recovers Eqs. (4.6–4.7).

## B Saddle point calculation of multiplicities

In this appendix, we analyze the large- $N$  asymptotic behavior of the summation formula from Eq. (5.27).

First, let us transform the summation into an integral representation by introducing the generating functions:

$$\mathcal{N}_n(\phi) := \sum_{d=-\infty}^{\infty} \mathcal{N}_n^d q^d \quad (q = e^{i\phi}), \quad (\text{B.1})$$

$$C^D(\phi_1, \dots, \phi_4) := \sum_{d_1, \dots, d_4=-\infty}^{\infty} C_{\vec{d}}^D q_1^{d_1} \dots q_4^{d_4}, \quad (q_\alpha = e^{i\phi_\alpha}), \quad (\text{B.2})$$

where we analytically continue  $\mathcal{N}_n^d$  and  $C_{d_1, \dots, d_4}^D$  to negative  $d$  according to Eqs. (5.19), (5.26). These generating functions can be found explicitly:

$$\mathcal{N}_n(\phi) = \left[ \begin{matrix} N \\ n \end{matrix} \right]_{q^2} q^{-n(N-n)} (q - q^{-1}), \quad (\text{B.3})$$

$$C^D(\phi_1, \dots, \phi_4) = 4\pi^3 \frac{\sin(D\phi_1)}{\sin^3(\phi_1)} (\delta_{2\pi}(\phi_1 - \phi_2) - \delta_{2\pi}(\phi_1 + \phi_2)) \dots (\delta_{2\pi}(\phi_1 - \phi_4) - \delta_{2\pi}(\phi_1 + \phi_4)), \quad (\text{B.4})$$

where  $\delta_{2\pi}(x) = \sum_{n \in \mathbb{Z}} \delta(x - 2\pi n)$ . Then Eq. (5.27) turns into an integral:

$$\begin{aligned} \text{Mult}_{N/2, \vec{n}}^D &= \sum_{d_\alpha > 0} C_{\vec{d}}^D \mathcal{N}_{\vec{n}}^{\vec{d}} = \frac{1}{2^4} \sum_{d_\alpha=-\infty}^{\infty} C_{\vec{d}}^D \mathcal{N}_{\vec{n}}^{\vec{d}} = \\ &= \frac{1}{2^4} \frac{1}{(2\pi)^4} \int_{-\pi}^{\pi} \dots \int_{-\pi}^{\pi} C^D(\vec{\phi}) \mathcal{N}_{n_1}(-\phi_1) \dots \mathcal{N}_{n_4}(-\phi_4) d\vec{\phi} = \\ &= \frac{1}{2\pi i} \oint \left[ \begin{matrix} N \\ n_1 \end{matrix} \right]_q \dots \left[ \begin{matrix} N \\ n_4 \end{matrix} \right]_q (q-1) q^{-\frac{\sum_\alpha n_\alpha (N-n_\alpha) + D+3}{2}} dq = V_{N, \vec{n}}^{+, D} - V_{N, \vec{n}}^{-, D}, \end{aligned} \quad (\text{B.5})$$

where the numbers  $V_{N, \vec{n}}^{\pm, D}$  are given by the following formula from Eq. (5.29):

The large- $N$  limit can be treated using a saddle point, located near  $q^* \simeq 1$ . Let us analyze the  $q$ -binomial coefficient near  $q = 1$ , expanding it in a Taylor series [31]:

$$\log \left[ \begin{matrix} M \\ n \end{matrix} \right]_{q=e^{\frac{2\pi x}{M+1}}} = \log \binom{M}{n} + \frac{\pi n(M-n)}{M+1} x + \sum_{s=1}^{\infty} \frac{(-1)^{s+1} \zeta(2s) A_{M,n}^{(s)}}{s(2s+1)} x^{2s}, \quad x \rightarrow 0, \quad (\text{B.6})$$

where  $A_{M,n}^{(s)} = \frac{B_{2s+1}(M+1) - B_{2s+1}(M-n+1) - B_{2s+1}(n+1)}{(M+1)^{2s}}$ ,  $B_n(x)$  denotes the  $n$ -th Bernoulli polynomial,  $\zeta(n)$  is a Riemann zeta function, and as  $0 < A_{M,n}^{(s)} < M+1$ , the absolute radius of convergence for the series is not less than 1.

Then, the saddle point  $x_\pm^*$  is defined as the solution to the following equation:

$$\sum_{s=1}^{\infty} \frac{(-1)^{s+1} \zeta(2s) A_{N, \vec{n}}^{(s)}}{2s+1} (x_\pm^*)^{2s-1} = \frac{\pi(D \mp 1)}{2(N+1)}, \quad (\text{B.7})$$

where  $A_{N, \vec{n}}^{(s)} = \sum_{\alpha} A_{N, n_\alpha}^{(s)}$ .

One can iteratively solve this equation as an expansion in powers of  $(N+1)^{-1}$ , but we restrict ourselves to the first order only, which leads to the approximation from Eq. (5.30). Substituting it into Eq. (B.5), we get the following approximation:

$$V_{N,\vec{n}}^{\pm,D} \approx \prod_{\alpha} \binom{N}{n_{\alpha}} \frac{2\pi}{N+1} \left( \frac{2\pi^3 \sum_{\alpha} n_{\alpha} (N - n_{\alpha})}{3(N+1)} \right)^{-1/2} \exp \left( - \frac{3(D \mp 1)^2}{2 \sum_{\alpha} n_{\alpha} (N - n_{\alpha}) (N+1)} \right). \quad (\text{B.8})$$

The multiplicity is given by the difference  $V_{N,\vec{n}}^{+,D} - V_{N,\vec{n}}^{-,D}$ . Noting that  $V_{N,\vec{n}}^{\pm,D}$  differ only by a  $\mp 1$  in the exponent, we can approximate the multiplicity by further expanding the exponent  $\exp \left( - \frac{3(D \mp 1)^2}{2 \sum_{\alpha} n_{\alpha} (N - n_{\alpha}) (N+1)} \right)$  in a Taylor series, arriving at Eq. (5.31).

## C Exact expression for the Jordan eigenvectors

In this section, we provide an expression for the Jordan canonical vectors of matrices  $h_l^{cl/q}$  introduced in Eqs. (5.11–5.12), through their adjugate matrices. Note that according to lemma 5.3, the linear envelope of these vectors provides a basis for the invariant subspaces of the matrix  $M$ .

For any matrix  $T$ , let us define the so-called adjugate matrix:

$$\text{Adj}(T) \stackrel{\text{def}}{=} (-1)^{i+j} \mathcal{M}_{i,j}(T), \quad (\text{C.1})$$

where  $\mathcal{M}_{i,j}(T)$  is the  $(j, i)$  minor of  $T$  and  $\text{Adj}(T) = \det(T)T^{-1}$  if  $T$  is invertible.

Now, for an arbitrary matrix  $A$  consider  $A(x) = \text{Adj}(x - A)$ . In this notation, the following useful theorem holds:

**Theorem C.1.** [32] *Let  $\lambda$  be an eigenvalue of  $A$  and  $n$  its algebraic multiplicity. Also, denote  $A_k(x) = \frac{1}{k!} \frac{d^k}{dx^k} A(x)$ . Then,*

$$(1) \quad (A - \lambda I)A_m(\lambda) = A_{m-1}(\lambda) \text{ for } m = 1 \dots n, \text{ and } (A - \lambda I)A_0(\lambda) = 0. \quad (\text{C.2})$$

$$(2) \quad \text{The root subspace of } A \text{ with eigenvalue } \lambda \text{ coincides with the image of } A_{n-1}(\lambda). \quad (\text{C.3})$$

This theorem implies that the vectors:

$$J_m = A_m(\lambda)|\Omega\rangle \quad (\text{C.4})$$

form a Jordan eigenbasis as long as  $A_n(\lambda)|\Omega\rangle \neq 0$ .

We apply this theorem to  $A = h_l^{cl/q}$ , defining  $h_l^{cl/q}(x) = \text{Adj}(x - h_l^{cl/q})$ . Since  $h_l^{cl}$  is lower triangular and  $h_l^q$  is upper triangular, we can immediately deduce that the highest vector of  $h_l^{cl}$  is obtained by taking  $\langle i|\Omega^{cl}\rangle = \delta_{i,1}$  and the highest vector of  $h_l^q$  requires  $\langle i|\Omega^q\rangle = \delta_{i,2N}$ .

All relevant components of the adjugate matrix take the following form:

$$\begin{aligned} (h_l^{cl}(x))_{2k-1,1} &= (x-1)^{N-k+1} x^{N-k} (s^2 + x - 1)^{k-1}, \\ (h_l^{cl}(x))_{2k,1} &= -s(x-1)^{N-k} x^{N-k} (s^2 + x - 1)^{k-1}, \end{aligned} \quad (\text{C.5})$$

$$\begin{aligned} (h_l^q(x))_{2N-2k+2,2N} &= \begin{cases} s^2(x-1)^{N-k} x^{N-k+1} (s^2 + x - 1)^{k-2}, & k > 1 \\ (x-1)^{N-1} x^N, & k = 1 \end{cases} \\ (h_l^q(x))_{2N-2k+1,2N} &= s(x-1)^{N-k} x^{N-k} (s^2 + x - 1)^{k-1}, \end{aligned} \quad (\text{C.6})$$



where  $s = \text{sech}(u)$ .

Substituting these formulas into the Eq. (C.4), we reproduce Eqs. (C.12).

As explained in Section (5.3), the IM might be created from the vacuum state  $|\Omega\rangle$  by the action of single-particle creation operators. Here we provide a proof that the Eq. (5.36) is compatible with the trace property of the IM from Eq. (2.6).

**Lemma C.2.** *The product of wave functions (5.33) satisfies the trace property of the IM (2.6).*

*Proof.* First, let us recall that the wave functions generate the eigenstates of a transfer matrix  $\tilde{T}$ , which is derived from the original TM by conjugation with a product  $\prod_{i=1}^{2N} \sigma_{2i-1}^y$ . In other words, the IM takes the following form:

$$\begin{aligned} \mathcal{I}_{s_1, \dots, s_{2N}}^{\bar{s}_1, \dots, \bar{s}_{2N}} &= \left( \prod_{j=1}^{2N} \sigma_{2j-1}^y \prod_{i=1}^N \Psi_{q,1,i}^\dagger \Psi_{cl,0,i}^\dagger |\Omega\rangle \right)_{\bar{s}_{2N}, \dots, \bar{s}_1, s_1, \dots, s_{2N}} = \\ &= (-1)^N \prod_{j=1}^N \bar{s}_{2N-2j+2} s_{2j-1} \prod_{i=1}^N \left( \Psi_{q,1,i}^\dagger \Psi_{cl,0,i}^\dagger |\Omega\rangle \right)_{-\bar{s}_{2N}, \bar{s}_{2N-1}, \dots, -\bar{s}_2, \bar{s}_1, -s_1, s_2, \dots, -s_{2N-1}, s_{2N}}. \end{aligned} \quad (\text{C.7})$$

Then it is apparent that taking the trace of the IM involves summation over singletons  $|\uparrow\downarrow\rangle - |\downarrow\uparrow\rangle$ . We now proceed to prove that the trace property holds. Start with rewriting the product of wave functions explicitly:

$$\begin{aligned} (-1)^N \prod_{i=1}^N \Psi_{cl,0,i}^\dagger \Psi_{q,1,i}^\dagger |\Omega\rangle &= \frac{(-1)^N}{(q^2 + 1)^N} \prod_{i=1}^N (J_{i,1}^{1,q} c_1^\dagger + \dots + J_{i,2N}^{1,q} c_{2N}^\dagger + J_{i,2N}^{1,q} c_{2N+1}^\dagger + \dots + J_{i,1}^{1,q} c_{4N}^\dagger) \times \\ &\quad \times (J_{i,1}^{0,cl} c_1^\dagger + \dots + J_{i,2N}^{0,cl} c_{2N}^\dagger - q^2 J_{i,2N}^{0,cl} c_{2N+1}^\dagger - \dots - q^2 J_{i,1}^{0,cl} c_{4N}^\dagger) |\Omega\rangle. \end{aligned} \quad (\text{C.8})$$

After that, one can notice that the ‘quantum’ part of the product is traceless, while the ‘classical’ part contributes to cancellations of  $(q^2 + 1)^N$ , since:

$$c_{i_1}^\dagger \dots c_{i_k}^\dagger c_1^\dagger c_{i_{k+1}}^\dagger \dots c_{i_{2N-1}}^\dagger |\Omega\rangle = (-1)^k \sigma_1^+ c_{i_1}^\dagger \dots c_{i_{2N-1}}^\dagger |\Omega\rangle, \quad (\text{C.9})$$

$$c_{i_1}^\dagger \dots c_{i_k}^\dagger c_{4N}^\dagger c_{i_{k+1}}^\dagger \dots c_{i_{2N-1}}^\dagger |\Omega\rangle = (-1)^k \sigma_{4N}^+ c_{i_1}^\dagger \dots c_{i_{2N-1}}^\dagger |\Omega\rangle. \quad (\text{C.10})$$

As a result, after taking a partial trace of the IM by  $s_{2N} = \bar{s}_{2N}$ , one comes up with the following reduced product (here formulas (5.35) play a crucial role):

$$\begin{aligned} \frac{(-1)^N}{(q^2 + 1)^{N-1}} (c_2^\dagger + c_{4N-1}^\dagger) \prod_{i=2}^N (J_{i,3}^{1,q} c_3^\dagger + \dots + J_{i,2N}^{1,q} c_{2N}^\dagger + J_{i,2N}^{1,q} c_{2N+1}^\dagger + \dots + J_{i,3}^{1,q} c_{4N-2}^\dagger) \times \\ \times (J_{i,3}^{0,cl} c_3^\dagger + \dots + J_{i,2N}^{0,cl} c_{2N}^\dagger - q^2 J_{i,2N}^{0,cl} c_{2N+1}^\dagger - \dots - q^2 J_{i,2}^{0,cl} c_{4N-2}^\dagger) |\Omega\rangle = \\ = (-1)^{N-1} (\sigma_2^+ - \sigma_{4N-1}^+) \prod_{i=2}^N \tilde{\Psi}_{q,1,i}^\dagger \tilde{\Psi}_{cl,0,i}^\dagger |\Omega\rangle, \end{aligned} \quad (\text{C.11})$$

which is nothing but a product of a singleton state with the IM, corresponding to  $N - 1$ . Thus, the proof is finished.  $\square$

## C.1 Local basis in Jordan cell

One way to obtain the wave functions belonging to each Jordan block is to examine the free-fermionic limit of the Bethe vectors, derived in section (4). Here we choose a different approach, to directly obtain the basis vectors,



applying the method of the adjugate matrix from [33]. Let us now focus on finding appropriate wave functions  $\Psi_{cl,0,k}^{+, \dagger}, \Psi_{q,1,k}^{+, \dagger}$ . One set of the Jordan vectors can be derived using the adjoint matrix, see the appendix (C):

$$\begin{aligned}\tilde{J}_{m,2k-1}^{0,cl} &= \frac{1}{(k-m)!} \partial_x^{k-m} \{(x-1)^{N+1-k} (s^2 - 1 + x)^{k-1}\} \Big|_{x=0}, \\ \tilde{J}_{m,2k}^{0,cl} &= -\frac{s}{(k-m)!} \partial_x^{k-m} \{(x-1)^{N-k} (s^2 - 1 + x)^{k-1}\} \Big|_{x=0}, \\ \tilde{J}_{m,2k-1}^{1,q} &= \frac{s}{(m-k)!} \partial_x^{m-k} \{x^{k-1} (s^2 - 1 + x)^{N-k}\} \Big|_{x=1}, \\ \tilde{J}_{m,2k}^{1,q} &= \frac{s^2}{(m-k)!} \partial_x^{m-k} \{x^k (s^2 - 1 + x)^{N-k-1}\} \Big|_{x=1},\end{aligned}\tag{C.12}$$

where  $s = \text{sech}(u)$  and  $k, m = 1 \dots N$ .

These formulas are not practical for computations, because they contain exponentially large values. To compute the IM, we are interested in linear envelopes  $\text{Span}(J_1^{0,cl}, \dots, J_N^{0,cl})$  and  $\text{Span}(J_1^{1,q}, \dots, J_N^{1,q})$ , rather than the Jordan blocks themselves.

A better choice of a basis, without exponentially large coefficients, is provided by the following formula:

$$\begin{aligned}J_{m,2k-1}^{0,cl} &= -\frac{1}{(k-m)!} \partial_x^{k-m} \{(x-1)^{m-k+1} (s^2 - 1 + x)^{k-m}\} \Big|_{x=0} = P_{k-m}^{(-2,0)}(1-2s^2) \\ J_{m,2k}^{0,cl} &= \frac{s}{(k-m)!} \partial_x^{k-m} \{(x-1)^{m-k} (s^2 - 1 + x)^{k-m}\} \Big|_{x=0} = s P_{k-m}^{(-1,0)}(1-2s^2), \\ J_{m,2k-1}^{1,q} &= \frac{s}{(m-k)!} \partial_x^{m-k} \{x^{k-m} (s^2 - 1 + x)^{m-k}\} \Big|_{x=1} = s P_{m-k}^{(0,-1)}(1-2s^2), \\ J_{m,2k}^{1,q} &= \frac{s^2}{(m-k)!} \partial_x^{m-k} \{x^{k-m+1} (s^2 - 1 + x)^{m-k-1}\} \Big|_{x=1} = P_{m-k}^{(-1,-1)}(1-2s^2),\end{aligned}\tag{C.13}$$

where  $P_k^{(\alpha,\beta)}(z)$  is a Jacobi polynomial:

$$\begin{aligned}P_k^{(\alpha,\beta)}(z) &= \frac{(-1)^k}{2^k k!} (1-z)^{-\alpha} (1+z)^{-\beta} \frac{d^k}{dz^k} \{(1-z)^\alpha (1+z)^\beta (1-z^2)^k\}, \quad k \geq 0 \\ P_k^{(\alpha,\beta)}(z) &\equiv 0, \quad k < 0\end{aligned}$$

One can see that such defined vectors are linear combinations of previously defined Jordan vectors:

$$\begin{aligned}J_{m,2k-1}^{0,cl} &= -\sum_{\tilde{m}=m}^k \frac{1}{(\tilde{m}-m)!} \partial_x^{\tilde{m}-m} \{(x-1)^{m-N} (s^2 - 1 + x)^{1-m}\} \Big|_{x=0} \tilde{J}_{\tilde{m},2k-1}^{0,cl}, \\ J_{m,2k}^{0,cl} &= -\sum_{\tilde{m}=m}^k \frac{1}{(\tilde{m}-m)!} \partial_x^{\tilde{m}-m} \{(x-1)^{m-N} (s^2 - 1 + x)^{1-m}\} \Big|_{x=0} \tilde{J}_{\tilde{m},2k}^{0,cl}, \\ J_{m,2k-1}^{1,q} &= \sum_{\tilde{m}=k}^m \frac{1}{(m-\tilde{m})!} \partial_x^{m-\tilde{m}} \{x^{1-m} (s^2 - 1 + x)^{m-N}\} \Big|_{x=1} \tilde{J}_{\tilde{m},2k-1}^{1,q}, \\ J_{m,2k}^{1,q} &= \sum_{\tilde{m}=k}^m \frac{1}{(m-\tilde{m})!} \partial_x^{m-\tilde{m}} \{x^{1-m} (s^2 - 1 + x)^{m-N}\} \Big|_{x=1} \tilde{J}_{\tilde{m},2k}^{1,q}.\end{aligned}\tag{C.14}$$

These new vectors  $|J_n^{0,cl}\rangle, |J_n^{1,q}\rangle$  do not provide a Jordan canonical basis, but they span the full root space. The

advantage of this new basis is a polynomial decay of the vector's components:

$$\begin{aligned}
 J_{1,2k-1}^{0,cl} &= \frac{1}{k^{1/2}} \left( \frac{s^3}{\pi \sqrt{1-s^2}} \right)^{1/2} \sin((2k-3) \arcsin(s) - 3\pi/4) + O(k^{-3/2}), \quad k \rightarrow \infty \\
 J_{1,2k}^{0,cl} &= \frac{1}{k^{1/2}} \left( \frac{s^3}{\pi \sqrt{1-s^2}} \right)^{1/2} \sin((2k-2) \arcsin(s) + 3\pi/4) + O(k^{-3/2}), \quad k \rightarrow \infty \\
 J_{N,2N-2k+1}^{1,q} &= \frac{1}{k^{1/2}} \left( \frac{s \sqrt{1-s^2}}{\pi} \right)^{1/2} \sin((2k-2) \arcsin(s) + \pi/4) + O(k^{-3/2}), \quad k \rightarrow \infty \\
 J_{N,2N-2k+2}^{1,q} &= \frac{1}{k^{1/2}} \left( \frac{s \sqrt{1-s^2}}{\pi} \right)^{1/2} \sin((2k-3) \arcsin(s) + 3\pi/4) + O(k^{-3/2}), \quad k \rightarrow \infty
 \end{aligned} \tag{C.15}$$

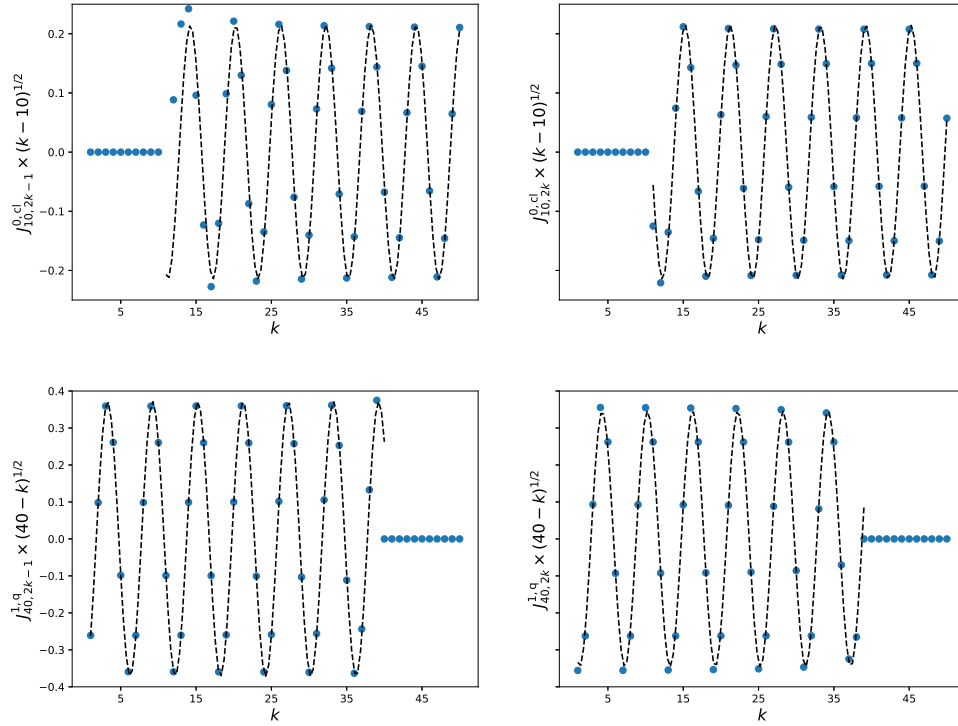


Figure 8: Components of  $|J_{10}^{0,cl}\rangle$  and  $|J_{40}^{1,q}\rangle$  for  $N = 50$ ,  $s = \frac{1}{2}$  together with their asymptotes, which are plotted as black dashed lines.

After we obtained explicit formulas for the basis components, it is straightforward to perform the Gram-Schmidt orthogonalization procedure, starting from the lowest vector  $J_N^{0,cl}$  (or  $J_1^{1,q}$ ). The resulting basis consists of vectors with the decay rate  $k^{-3/2}$ . We were not able to find the general formula for the components. However, numerical studies provide the conjecture for the asymptotics 5.38.